

THE APPLICATION OF THE MM5 TO TROPICAL CYCLOGENESIS AT CLOUD-RESOLVING RESOLUTION

Jordan G. Powers and Christopher A. Davis
National Center for Atmospheric Research,*
Boulder, Colorado

1. INTRODUCTION

One of the main challenges remaining in the study of tropical cyclones is understanding and predicting their genesis, especially the development of organized cloud clusters (*i.e.*, one or more mesoscale convective systems (MCSs)) into a warm core vortex. The difficulty in making progress in this area has reflected the genesis process involving three scales of motion (cloud, mesoscale, and synoptic scale) and the need to observe each of these in detail, from upscale growth and intensification of a complex, dispersed system into a single, coherent vortex.

Most modeling studies of tropical cyclogenesis have been restricted to grid spacing too coarse to resolve convective cells (Davis and Bosart 2001) (hereinafter DB1), or if not, have mainly considered mature hurricanes (Liu *et al.* 1997; Braun 2002). Moreover, they have imposed a vortex at the initial time and have not employed cloud-resolving grid spacing (*i.e.*, 2 km or less) for the entire simulation over scales capturing the synoptic environment. This study is thus in large part driven by the issue of whether a mesoscale model (in particular, the MM5) can realistically capture tropical cyclogenesis by applying high resolution over a broad, synoptically-defined region before any tropical system signature is present.

To address this, a high-resolution MM5 simulation of the development of Tropical Cyclone Diana (1984) is performed in a study that is unprecedented in a combination of three ways:

(i) the use of cloud-resolving grid spacing for the entire simulation;

(ii) no imposed mesoscale vortex in the initial condition; and

(iii) a domain large enough to capture both the storm and the response of the environment to deep convection.

This paper presents the key results of this investigation.

2. METHODOLOGY

The MM5 (Grell *et al.* 1995) is used here with a 1.2-km horizontal grid of regional-scale area (1272 km \times 1200 km) for the period of Diana's formation from 0000 UTC 8 September–0000 UTC 10 September 1984. The area of the grid is outlined by the box in Fig. 1(b). 37 half- σ levels from the surface to 50 hPa are employed. There is no vortex bogussing in the initial conditions, nor are nested domains used. Given the grid size, the MM5 is run fully-explicit, with the Reisner 2 scheme being active. The PBL parameterization is the MRF scheme.

The initial conditions (ICs) for 0000 UTC 8 Sept were derived from NCEP/NCAR analyses objectively reanalyzed with the available observations via Little-r. This was done in the context of the 27-km MM5 Diana simulation of DB1. The ICs were interpolated from such 27-km grid to the 1.2-km domain. In part, the DB1 27-km grid was used to provide a relatively smooth IC, one lacking significant mesoscale detail. Figure 1 shows these initial conditions.

Figure 1(a) presents the upper-level (340 K isentropic surface) flow and potential vorticity (PV) distribution, and a longwave trough over the genesis region (east of Florida) is apparent. Figure 1(b) offers the low-level (850 hPa) conditions, with general easterlies north of the Bahamas driven by an anticyclone centered to the north. Implied is significant vertical shear over the genesis area. The baroclinic zone reflects a remnant stationary front along which is present a weak baroclinic low.

3. RESULTS

In Diana's evolution into a tropical storm, she tracked generally west-northwestward toward the central Florida coast from north of the Bahamas (see DB1). As

* The National Center for Atmospheric Research is sponsored by the National Science Foundation.

Corresponding author address: Dr. Jordan G. Powers, MMM Division, NCAR, P.O. Box 3000, Boulder, CO 80307-3000.
email: powers@ncar.ucar.edu

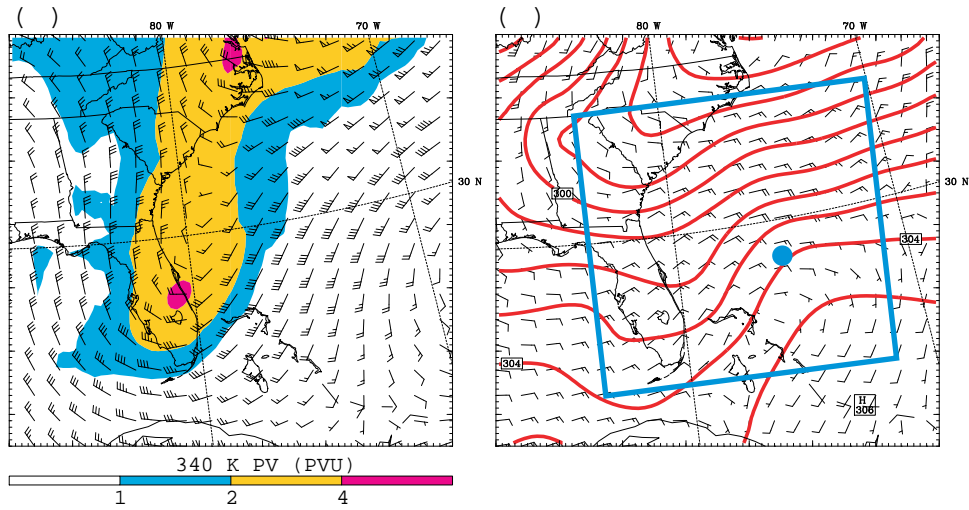


Figure 1. (a) Ertel PV and wind on the 340K isentropic surface at 0000 UTC 8 Sept 1984. Fields here from the 27-km grid used in DB1, with winds shown every three grid points. PV units shaded. (b) Wind and θ (interval= 1K) on the 850 hPa surface. Solid box denotes boundary of the 1.2-km grid used for the simulation. Dot marks center of the original MCS and MCV.

shown in Fig. 2, model storm intensity, as measured by the minimum SLP, was weaker than that analyzed through the simulation period. In better agreement with observation (see, *e.g.*, DB1), however, the simulation exhibited three stages of deepening: (i) widespread deep convection and initial MCS and vortex formation; (ii) significantly decreased convection and rainfall; and (iii) renewed convection and warm-core vortex intensification. These are reflected in Fig. 2's time series of central SLP and of hourly rainfall averaged over a 150 km \times 150 km area centered on the storm. The first stage appears in the SLP decrease and rainfall increase and maximum through about hour 15; the second phase, of decreased convection and static SLP, follows and extends to about hour 25; the third phase, marked by increasing rain and falling SLP, then runs to the end of the simulation.

In phase one, mesoscale destabilization due to ascent and lower-tropospheric warm advection (associated with the remnant front) lead to a convective outbreak around hr 9. This was centered around 28.3N, 75W and is marked by the dot in Fig. 1(b). An MCS emerged, and by 1200 UTC 8 Sept (hr 12) a cyclonic vortex of 50–60 km radius had begun to form on the southwestern periphery of the system's stratiform region. Figure 3 shows this, while Fig. 2 indicates the relatively high precipitation rate in this period. From about hr 15, however, the MCS decayed, and the mesoscale convective vortex (MCV) weakened. It did not dissipate entirely, though, and eventually re-intensified into Tropical Storm Diana.

The major dropoff in rainfall at about hr 15 (Fig. 2) marked the transition to the approximately 10-hour quiescent period of development. Convection diminished during this phase in connection with PBL drying associated with downward mesoscale motion over the region. For example, the 900–800 hPa average RH (over a vortex-centered, 150 km \times 150 km area) fell from 92.4% to 83.0% entering the quiescent phase; thereafter, in re-intensification, it rose back to 92.8%. Analyses

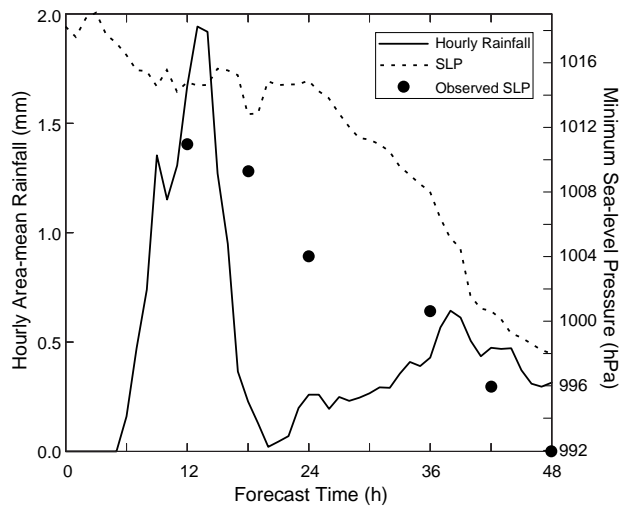


Figure 2. Time series of simulated minimum SLP (lighter, decreasing curve) and observed SLP (dots), and storm-centered, hourly rainfall averaged over a 150 km \times 150 km area (darker curve).

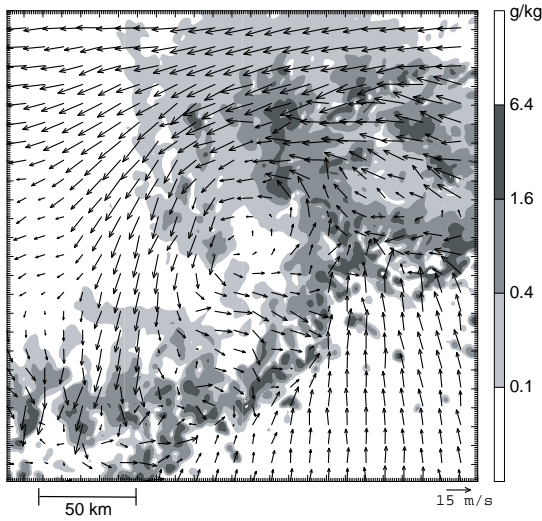


Figure 3. Rain water mixing ratio (shaded; $g\ kg^{-1}$) and wind at 1 km MSL (~ 900 hPa) at 15 h (1500 UTC 8 Sept). Window area $\sim 300\ km \times 300\ km$.

of non-linear balanced vertical velocity obtained by inverting Ertel PV revealed that the subsidence in part resulted from tilting of the deep vortex (formed by the initial MCS) by the vertically-sheared background flow.

The transition from this period of quiescence to that of final re-intensification was marked by PBL moistening and renewed rainfall, primarily northeast of the cyclone center. After hr 34, significant convection erupted on the southwest flank of the vortex. As shown in

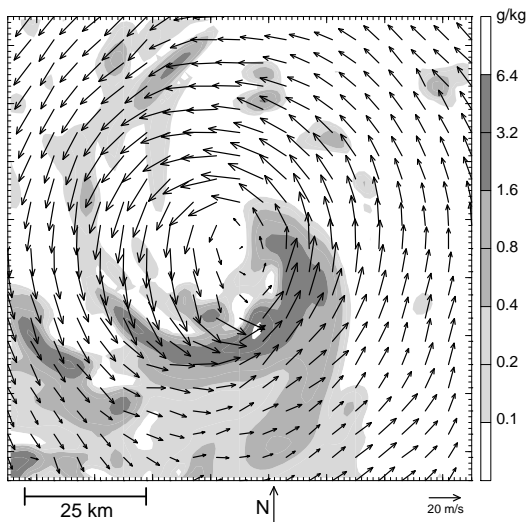


Figure 4. Rain water mixing ratio (shaded; $g\ kg^{-1}$) and wind at 1 km MSL (~ 900 hPa) at 40 h (1600 UTC 9 Sept). Window area $\sim 95\ km \times 95\ km$.

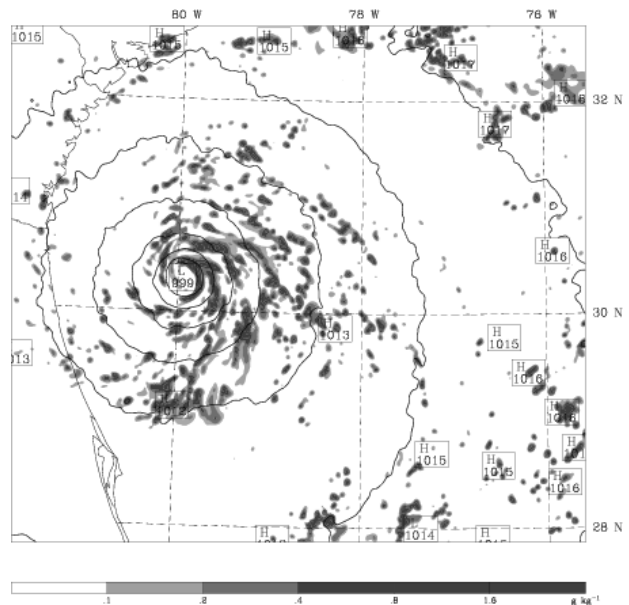


Figure 5. SLP (interval= 2 hPa) and rain water mixing ratio (shaded; $g\ kg^{-1}$) at 900 hPa at 48 h (0000 UTC 10 Sept). 500 \times 450 window of full 1060 \times 100 grid pt. domain shown.

Fig. 4, by hr 40 this organized into a comma-shaped rainband with an intensification of westerly winds (to $\sim 20\ ms^{-1}$) on the southern side of the vortex. The intense rainband began to close off the circulation center and was attended by the relatively rapid fall of central pressure (see Fig. 2). This development was facilitated by a reduction and reorientation of the vertical shear. Specifically, from the middle of the quiescent period the .5–3.5 km vertical shear decreased from about $12\ ms^{-1}$ directed northeasterly to approximately $2\text{--}3\ ms^{-1}$ directed southwesterly to southerly.

Throughout the storm's development, the high-resolution MM5 was able to simulate the evolution of individual convective elements into bands. Figure 5 presents a snapshot of the mature structure of simulated T.S. Diana off the Florida coast at hr 48, with the MM5 capturing both individual cells and spiral bands. While the smallest resolvable features are produced, realistic upscale organization also occurs, and such behavior is repeatedly seen throughout the simulation.

4. SUMMARY

This study has investigated the genesis of tropical cyclone Diana (1984) using the MM5 run at cloud-resolving (1.2-km) resolution over a regional-scale domain. The MM5 was initialized with only synoptic information depicting a weak baroclinic system on a

stationary front. There was no use of nested domains, and there was no bogus vortex insertion into the ICs.

The MM5 realistically captures the formation of Diana and its progression through three stages of deepening: initial convection, quiescence, and re-intensification. It is found that with a large, cloud-resolving grid the MM5 can recreate tropical cyclogenesis, and, in particular, the organization of classic spiral bands from distinct, resolved convective cells can be reproduced.

REFERENCES

- Braun, S.A., 2002: A cloud-resolving simulation of Hurricane Bob (1991): Storm structure and eyewall buoyancy. *Mon. Wea. Rev.*, **130**, 1573–1592.
- Davis, C.A. and L.F. Bosart, 2001: Numerical simulations of the genesis of Hurricane Diana. Part I: Control simulation. *Mon. Wea. Rev.*, **129**, 1859–1881.
- Grell, G.A., J. Dudhia, and D.R. Stauffer, 1995: *A Description of the Fifth-Generation Penn State/NCAR Mesoscale Model (MM5)*, NCAR Tech. Note TN-398+STR, 122 pp.
- Liu, Y., D.-L. Zhang, and M.K. Yau, 1997: A multiscale numerical study of Hurricane Andrew (1992). Part I: Explicit simulation and verification. *Mon. Wea. Rev.*, **125**, 3073–3093.